PHYSICAL MODELING OF THE OUTER BELT HIGH ENERGY ELECTRONS

D. Boscher, S. Bourdarie

ONERA-CERT/DESP, 2. Av. E. Belin, BP 4025, 31055 Toulouse Cedex 4, France

ABSTRACT

We tried to reproduce the dynamics of the outer radiation belt during magnetic storms with Salammbô-3D. Using dynamic Meteosat-3 spectra as boundary conditions, different runs were performed and the results compared to CRRES-MEA data. Time dependent radial diffusion coefficients and plasmapause location gave the best results, only driven by the magnetospheric index Kp . From the results, it appears that the physics of the dynamic transport process of high energy electrons during perturbed period is well understood, but it seems that some empirical models (wave characteristics, low energy particles) have to be refined to improve the model.

1. INTRODUCTION

Reproducing the dynamics of the electron belt by a physical model during magnetic storms is not a easy task. Even it is supposed that all the physical phenomena leading to the transport and losses of particles are well modeled, their parameters can vary during storms, in particular during main phase and recovery phase. Moreover, non linearity can occur due to these evolving parameters, in addition to non linear process like the recirculation one (Ref. 1). The aim of this study is to understand the influence of some parameters on the electron transport, in particular in the outer zone.

To see this influence, the Salammbô-3D electron code (Ref. 2) was used. In this classical diffusion code, radial transport is the main process which carry particles from the outer boundary to the electron belt. During their transport, particles can interfere with different bands of waves (VLF transmitters, whistlers and plasmaspheric hiss) which can change their pitch angles. Friction and pitch angle diffusion by Coulomb interactions are acting at low altitude to precipitate electrons into the high atmosphere. During storm periods, different process can modify this steady picture of the slow transport and precipitation of electrons in the inner magnetosphere. First of all, injections occur near synchronous orbit, increasing the number of particles which can be transported. Then, radial transport is directly related to the perturbation of the electric and magnetic fields, which vary strongly during storms. The flow of particles carried from the external boundary to the inner magnetosphere can then be greatly enhanced. Finally, characteristics of the waves, in particular plasmaspheric hiss, can be greatly modified in some regions of space, like near the plasmapause.

2. MODELING THE SEPTEMBER-OCTOBER 1991 STORM PERIOD

We wanted to see the influence of some of these parameters. To do that, different runs of Salammbô were performed to compare with CRRES MEA measurements between the September 24 and the October 7, 1991. This period was magnetically very disturbed (see figure 1), with a Kp up to 7 and a Dst around –160 nT on October 1st and 2nd. As the dynamics of the electrons can be greatly influenced by the initial conditions, a particular attention was placed on it. At low energies (between 1 keV and 111 keV), this initial condition was deduced from a first run of Salammbô with steady parameters. At MEA energies (between 111 keV and 1581 keV), measurements of MEA during the first half of the 1025th orbit were used, and for higher energies, the initial state was deduced from the NASA AE8 MAX model. As for the boundary conditions (fixed in the code at L = 7), we used at low energies a steady spectrum deduced from ATS6 measurements, and at higher energies (between 43 keV and 300 keV) the time dependent measurements of the Meteosat-3 synchronous satellite. These fluxes were directly used in spite of the difference between day and night measurements (due to the asymmetry of the magnetic field), integration being made by the radial transport itself.

The first run was performed using constant standard radial diffusion coefficients (D_{LL}) and plasmapause location, which corresponds to the upper boundary for the plasmaspheric hiss in the code (L = 4.5). Comparing the obtained results to the measurements, not enough particles were found, in particular in the slot region (see figure 1) in the 100 keV range. Increasing the D_{LL}s by a factor of 5, particles can be better transported from the boundary down to L = 4, as seen in figure 1. Nevertheless, the particle flow is not sufficient to obtain enough particles at the end of the simulation, and the dynamics does not reproduce what is seen on board the CRRES satellite.

But it seems obvious that during storms radial diffusion coefficients can be greatly increased, as they follow the perturbations of the electric and magnetic fields. A Kp dependence of these coefficients was modeled and gave good results for the comparison between CRRES MEB low energy proton (around 100 keV) measurements and Salammbô-2D results (ref. 3) during all the CRRES life. The same Kp dependence was used here for electrons, i.e. exp(0.74Kp). The results are shown on the figure 1. They better fit the measurements, in particular for the first storm with a Kp value of 6 which give in the simulation an increase of the fluxes by a factor of 3. Nevertheless, this increase is not sufficient as compared to the measurements. This can either be due to the initial populations in particular at lower energies (note the difference between the initial conditions at this energy and this L value and measurements), or the dependence of the D_{LL}s, in L, energy or Kp. Another dynamic effect can also be of great influence on the fluxes, the plasmapause location evolution. In effect, during storms, plasmapause moves inward, following the increase in the electric fields. As it moves, hiss cannot propagate anymore outside the plasmasphere and involve the pitch angle diffusion of the electrons. Following Carpenter and Anderson (ref 4), we used their relationship: $Lpp = 5.6 - 0.46Kp_{max}$ to relate the maximum value of Kp during the 24 preceding

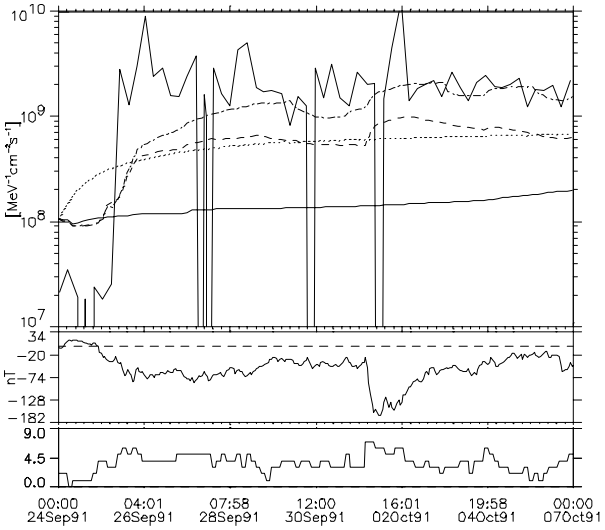

Figure 1. The September 24, 1991 storm: Kp (lower panel), Dst (middle panel), around 100 keV omnidirectional fluxes in the L = 4 region from CRRES-MEA (noisy solid curve), from Salammbô using standard (solid line), 5 times standard (dotted line), Kp dependent (dotted and dot-dashed lines) radial diffusion coefficients, the dot-dashed line being also with a Kp dependent plasmapause location.

hours, ignoring the values in the preceding hour. The results of this calculation, using Kp dependent D_{LL}s and plasmapause location, is also shown on figure 1. Comparison is better, though the increase in the first storm is not sufficient. Nevertheless, an increase in the fluxes by a factor of 10 is then obtained during the whole period. Globally, it seems from the simulation that, if all the other parameters are correct, radial diffusion coefficients would be more efficient than calculated for such energy and L values.

The results in this last case for different energies and all L values are plotted as grey coded omnidirectional fluxes in a L versus time grid on plate 1. The nearly 100 keV electron fluxes, from which the figure 1 is extracted, are plotted on panels 3 and 4 from the bottom, the 3rd being from CRRES-MEA measurements and the 4th from the code results. Injections are seen in the Salammbô results near the L = 7 boundary; they are related to the Meteosat-3 measurements shown on the top panel in an energy versus time grid. It seems from the comparison between these two panels the filling of the slot region is too slow with the code, as already seen in figure 1, but too much particles are transported near the inner belt at the end of the period. Nevertheless, the absolute values are not too different, in spite of the non intercalibration between Meteosat-3 (the input boundary) and CRRES-MEA(the output comparison). For nearly 400 keV (5th and 6th panels from the bottom), the comparison is better, excepted during the storm periods when magnetic field disturbances are strong. For the highest energy (around 1600 keV, 7th and 8th panels from the bottom), calculated particles are too much inside the magnetosphere. Nevertheless, the absolute values are not too different; maybe a change in the wave characteristics would imply a different result at this energy, due to the resonance effect between particles and waves. To conclude for this storm period, it seems that taking into account Kp dependent D_{LL}s and plasmapause location gave dynamic results which begin to really look like measurements.

3. RESULTS FOR THE OCTOBER 1990 STORM PERIOD

Then, other storm periods were studied. The same code including Kp dependent D_{LL}s and plasmapause location was run during another period of magnetic activity, i.e. the period between the October 8 and the October 21, 1990, with a storm reaching a value of 6 for Kp and around –130 nT for Dst on October 10. The results are plotted in the same plate 1 format in plate 2. Once more, the results at low energy fit relatively well to the measurements, but now, it is clear that at medium energy (near 400 keV), too much particles are transported near L = 4 during the whole period. This can be due to the recycling process, which does not compensate enough the particle loss in this region of the phase space. It is certainly related to the wave spectrum, which cannot be accurate for the frequencies resonating with that particles in this region. It can also be due to the dynamics of the waves (ref. 5).

4. CONCLUSION

The physical code Salammbô-3D including Kp dependent D_{LL}s and plasmapause location was implemented. From the results, it seems that these two effects have a great influence on the dynamics of the electrons in the 100 keV-1 MeV range. With this "simple" model only depending on the magnetospheric index Kp (but some boundary conditions were taken from measurements on board Meteosat-3) it was possible to reproduce two periods of magnetic activity. The difference between the simulation results and measurements (from CRRES-MEA) can be attributed to: 1) non accurate initial conditions, especially at low energies (< 100 keV), 2) non accurate dynamic spectrum at low energy (<50 keV) at the boundary condition, 3) uncertainties in the wave spectrum and possibly to its dynamics during storms, and 4) inaccurate radial diffusion coefficients. Moreover, with evolving parameters, the classical diffusion equation becomes non linear. Then, the response of the electrons can be due to rapidly varying parameters, faster than the three-hour Kp index.

5. REFERENCES

1. Boscher, D & al 1998, Influence of the wave characteristics on the electron radiation belt distribution, 32nd COSPAR Assembly, Nagoya (Japan), 12-19 July 1998.
2. Beutier, T & Boscher D 1995, A three-dimensional analysis of the electron radiation belt by the Salammbô code, *J. Geophys Res*., 100, 14853-14861.
3. Bourdarie, S & al 1996, A physics based model of the radiation belt flux at the day timescale, *ESA Publications SP-392*, 159-163.
4. Carpenter DL & Anderson RR 1992, An ISEE/whistler model of equatorial electron density in the magnetosphere, *J. Geophys Res*., 97, 1097-1108.
5. Smith EJ &al 1974, Plasmaspheric hiss intensity variations during magnetic storms, , *J. Geophys Res*., 79, 2507-2510.

ACKNOWLEDGMENTS
This work was supported under ESA grant number 11711/95/NL/JG. Plates presented in this paper make use of the PAPCO data analysis package supported by MPAe Lindaü through the Max-Planck-Gesellschaft, DARA grant 50 OC 95010, and as part of the HYDRA NASA funding under grant number NAG 5 2231.

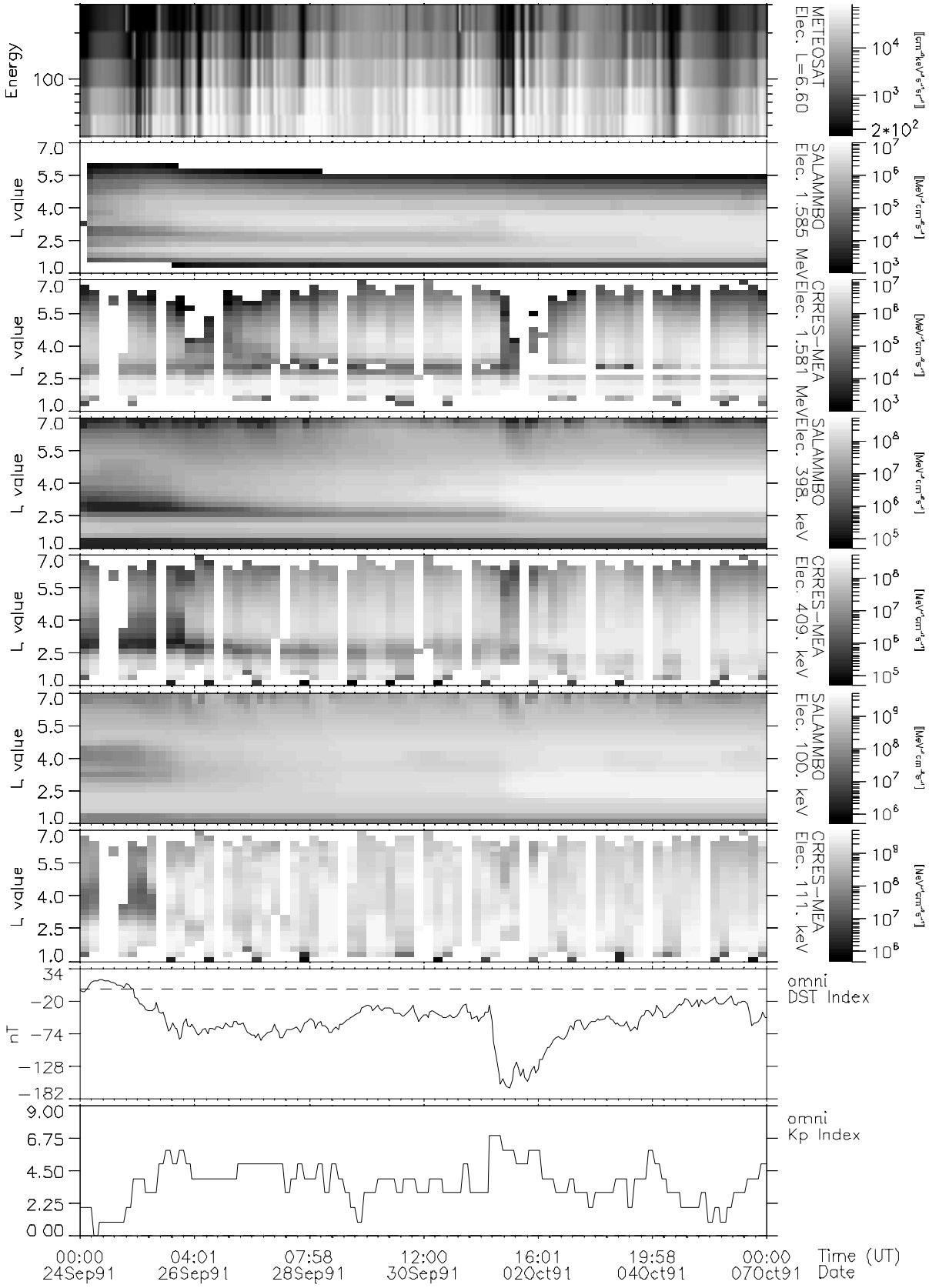

Plate1. Comparison between measurements and simulation for the September 24-October 7, 1991 period: Kp and Dst (first and 2nd panels from the bottom), CRRES-MEA and Salammbô for nearly 100 keV (3rd and 4th panels), for around 400 keV (5th and 6th panels), and for around 1600 keV (7th and 8th panels), and Meteosat-3 measurements (9th panel, at the top), used as boundary conditions for the simulation.

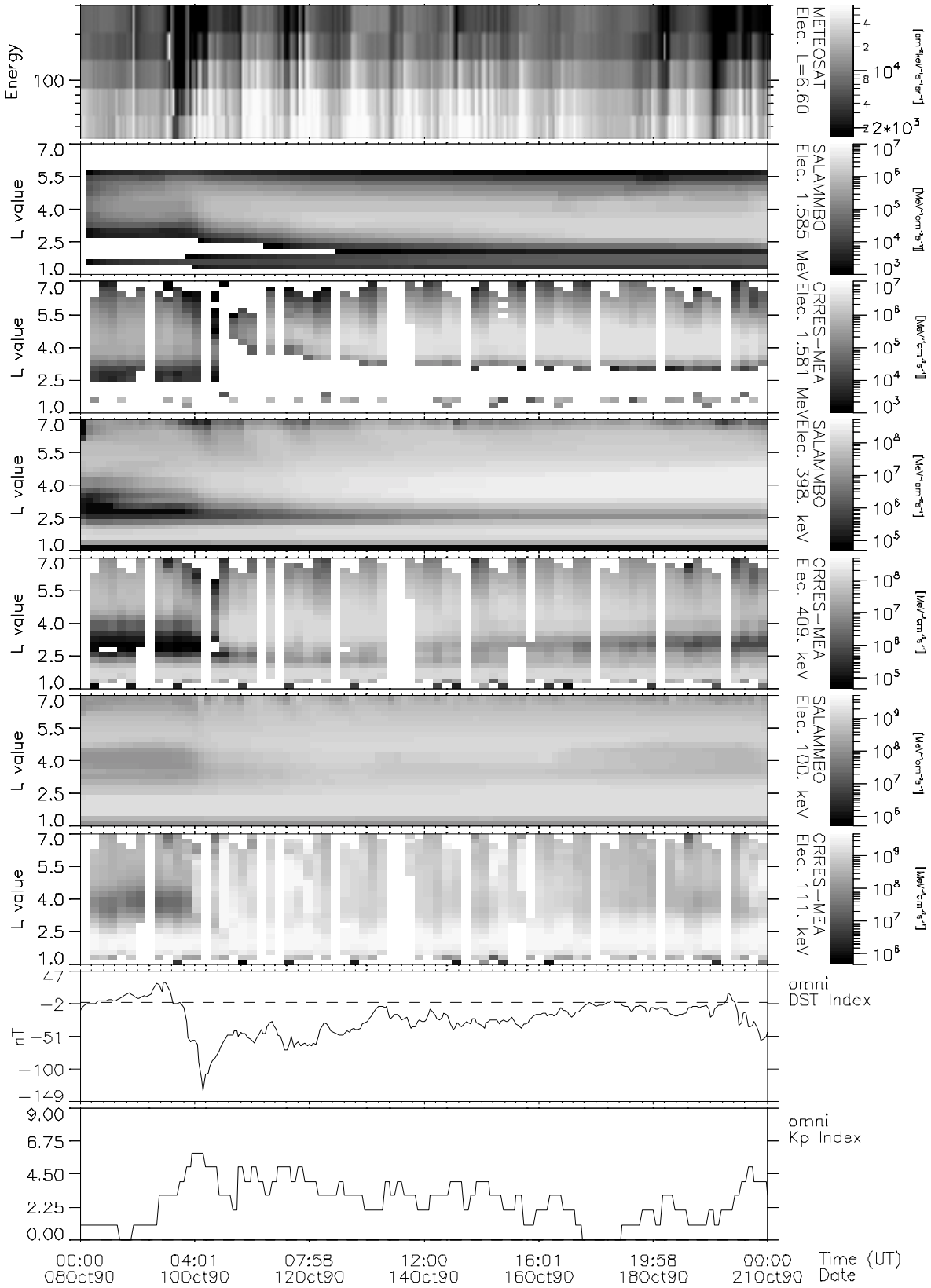

Plate2. Comparison between measurements and simulation for the October 8-October 21, 1990 period: Kp and Dst (first and 2nd panels from the bottom), CRRES-MEA and Salammbô for nearly 100 keV (3rd and 4th panels), for around 400 keV (5th and 6th panels), and for around 1600 keV (7th and 8th panels), and Meteosat-3 measurements (9th panel, at the top), used as boundary conditions for the simulation.